8-9-2018

Identification of enhanced IFN-γ signaling in polyarticular juvenile idiopathic arthritis with mass cytometry

Allison A Throm
Washington University School of Medicine in St. Louis

Halima Moncrieffe
University of Cincinnati

Amir B Orandi
Washington University School of Medicine in St. Louis

Jeanette T Pingel
Washington University School of Medicine in St. Louis

Theresa L Geurs
Washington University School of Medicine in St. Louis

See next page for additional authors

JCI insight

Identification of enhanced IFN-γ signaling in polyarticular juvenile idiopathic arthritis with mass cytometry

Allison A. Throm, … , Stephen T. Oh, Anthony R. French

JCI Insight. 2018;3(15):e121544. https://doi.org/10.1172/jci.insight.121544.

Research Article | Immunology | Inflammation

Polyarticular juvenile idiopathic arthritis (JIA) is among the most challenging of the JIA subtypes to treat. Even with current biologic therapies, the disease remains difficult to control in a substantial subset of patients, highlighting the need for new therapies. The aim of this study was to use the high dimensionality afforded by mass cytometry with phospho-specific antibodies to delineate signaling abnormalities in immune cells from treatment-naive polyarticular JIA patients. Peripheral blood mononuclear cells were isolated from 17 treatment-naive polyarticular JIA patients, 10 of the patients after achieving clinical remission, and 19 healthy controls. Samples were stimulated for 15 minutes with IL-6 or IFN-γ and analyzed by mass cytometry. Following IFN-γ stimulation, increased STAT1 and/or STAT3 phosphorylation was observed in subsets of CD4 T cells and classical monocytes from treatment-naive patients. The enhanced IFN-γ signaling was associated with increased expression of JAK1 and SOCS1 in CD4 T cells. Furthermore, substantial heterogeneity in surface marker expression was observed among the subsets of CD4 T cells and classical monocytes with increased IFN-γ responsiveness. The identification of enhanced IFN-γ signaling in CD4 T cells and classical monocytes from treatment-naive polyarticular JIA patients provides mechanistic support for investigations into therapies that attenuate IFN-γ signaling in this disease.

JCI insight

RESEARCH ARTICLE

Identification of enhanced IFN-γ signaling in polyarticular juvenile idiopathic arthritis with mass cytometry

Allison A. Throm,[1,2] Halima Moncrieffe,[3,4] Amir B. Orandi,[1] Jeanette T. Pingel,[1] Theresa L. Geurs,[1] Hannah L. Miller,[5] Allyssa L. Daugherty,[1] Olga N. Malkova,[6] Daniel J. Lovell,[7] Susan D. Thompson,[3] Alexei A. Grom,[7] Megan A. Cooper,[1] Stephen T. Oh,[6,8] and Anthony R. French[1,2,5]

[1]Division of Pediatric Rheumatology, Department of Pediatrics, Washington University School of Medicine, St. Louis, Missouri, USA. [2]Department of Biomedical Engineering, Washington University in St. Louis, St. Louis, Missouri, USA. [3]Center for Autoimmune Genomics and Etiology, Cincinnati Children's Hospital Medical Center, Cincinnati, Ohio, USA. [4]Department of Pediatrics, University of Cincinnati, College of Medicine, Cincinnati, Ohio. [5]Department of Pathology and Immunology and [6]The Andrew M. and Jane M. Bursky Center for Human Immunology and Immunotherapy Programs, Washington University School of Medicine, St. Louis, Missouri, USA. [7]Division of Rheumatology, Cincinnati Children's Hospital Medical Center, Cincinnati, Ohio, USA. [8]Division of Hematology, Department of Internal Medicine, Washington University School of Medicine, St. Louis, Missouri, USA.

Polyarticular juvenile idiopathic arthritis (JIA) is among the most challenging of the JIA subtypes to treat. Even with current biologic therapies, the disease remains difficult to control in a substantial subset of patients, highlighting the need for new therapies. The aim of this study was to use the high dimensionality afforded by mass cytometry with phospho-specific antibodies to delineate signaling abnormalities in immune cells from treatment-naive polyarticular JIA patients. Peripheral blood mononuclear cells were isolated from 17 treatment-naive polyarticular JIA patients, 10 of the patients after achieving clinical remission, and 19 healthy controls. Samples were stimulated for 15 minutes with IL-6 or IFN-γ and analyzed by mass cytometry. Following IFN-γ stimulation, increased STAT1 and/or STAT3 phosphorylation was observed in subsets of CD4 T cells and classical monocytes from treatment-naive patients. The enhanced IFN-γ signaling was associated with increased expression of JAK1 and SOCS1 in CD4 T cells. Furthermore, substantial heterogeneity in surface marker expression was observed among the subsets of CD4 T cells and classical monocytes with increased IFN-γ responsiveness. The identification of enhanced IFN-γ signaling in CD4 T cells and classical monocytes from treatment-naive polyarticular JIA patients provides mechanistic support for investigations into therapies that attenuate IFN-γ signaling in this disease.

Introduction

Polyarticular juvenile idiopathic arthritis (JIA) represents a subset of JIA patients with arthritis involving 5 or more joints, beginning before 16 years of age, without features of psoriatic arthritis or a spondyloarthropathy. Polyarticular JIA constitutes approximately 15%–25% of JIA patients and can be further subdivided based on the presence or absence of rheumatoid factor (RF) (1, 2). The incidence of polyarticular JIA in the US has been reported to be 2 per 100,000 people (3). Polyarticular JIA inflicts significant morbidity on children, including joint limitation and/or destruction. For example, a high percentage of hand and wrist x-rays from polyarticular JIA patients identify abnormalities at the time of diagnosis (4), and 50% of patients manifest evidence of radiographic progression within 2 years of diagnosis (5).

Prior to the advent of biologic agents, polyarticular JIA was often refractory to therapy, with only 6%–23% of patients achieving long-term remission at 10 years (6, 7) and with those with RF^+ polyarticular JIA being the least likely to sustain remission off medications of all JIA subsets (8). Even with modern biologic therapies, a significant fraction of polyarticular JIA patients have persistent disease activity (9). RF^+ polyarticular JIA patients in particular have lower response rates to treatment and longer times to clinical remission, with higher rates of disease flare (8, 10, 11). Together, these observations suggest mechanistic differences in polyarticular JIA compared with other JIA subsets.

Conflict of interest: The authors have declared that no conflict of interest exists.

Submitted: April 9, 2018
Accepted: June 28, 2018
Published: August 9, 2018

Reference information:
JCI Insight. 2018;3(15):e121544.
https://doi.org/10.1172/jci.insight.121544.

Overall, the etiology of JIA is not well characterized. Siblings of patients with JIA are over 15-fold more likely to develop JIA than the general population (12), with monozygotic twins having an even higher concordance rate of 25%–40% for JIA (13), implicating a genetic component to the disease. However, minimal evidence exists for a Mendelian pattern of inheritance, suggesting that JIA is a complex disorder associated with multiple genes. The strongest genetic association is with HLA alleles (1, 2), accounting for 13%–20% of the sibling concurrence risk in JIA and implicating T cell involvement in disease (12, 14). Furthermore, cellular infiltrates in affected joint synovium are enriched for T cells as well as B cells and macrophages (1). There is also accumulating evidence that innate immune responses contribute to the onset of polyarticular JIA (15–18). For example, a study of transcriptional profiles of peripheral blood mononuclear cells (PBMCs) from polyarticular JIA patients (prior to therapy with methotrexate or biologic agents) identified the upregulation of monocyte-associated and plasmacytoid dendritic cell–associated genes in subsets of polyarticular JIA patients (19).

The strong upregulation of inflammatory cytokines in polyarticular JIA patients has provided additional insight into the pathogenesis of polyarticular JIA. IL-6 is upregulated in the sera and synovial fluid of polyarticular JIA patients and correlates with severity of joint involvement and inflammatory markers (20). A multiplex survey of 30 cytokines and chemokines in the plasma and synovial fluid of polyarticular JIA patients demonstrated that IL-1, IL-6, IFN-γ, and, to a lesser extent, TNF-α were strongly upregulated in the plasma of polyarticular JIA patients with active compared with quiescent disease (21). Biologic agents specifically targeting IL-1, IL-6, and TNF-α have been shown to be efficacious in treating polyarticular JIA in randomized controlled trials (22–27), highlighting the importance of inflammatory cytokines in the pathogenesis of polyarticular JIA.

Despite the insights gained in previous studies and the success of a number of biologic agents that block proinflammatory cytokines, a subset of polyarticular JIA patients have difficult to control, refractory disease. Therefore, to further investigate potential immune cell signaling perturbations in polyarticular JIA patients, we performed mass cytometry on PBMCs from treatment-naive polyarticular JIA patients and controls. By coupling the deep profiling allowed by mass cytometry with multiparameter phospho-specific antibodies, we were able to probe the activation state of 14 signaling molecules in 13 distinct leukocyte subsets within single patient samples both at baseline and following perturbations with IFN-γ or IL-6. This approach identified enhanced IFN-γ responsiveness in subsets of CD4 T cells and monocytes from treatment-naive polyarticular JIA patients.

Results

Patient cohort. Samples from 17 treatment-naive polyarticular JIA patients, 10 of the 17 JIA patients while in clinical remission on medication, and 19 controls were analyzed (Table 1). Patients who had either not achieved clinical remission at the time of the analysis or for whom follow-up samples were not available were not included in the assessment of samples in clinical remission on medication. The age of the patients and controls in the cohort was well matched with a mean patient age of 11.6 years and mean control age of 11.7 years. 52.9% of the patients were female, while 73.7% of the controls were female.

Immune cell percentages. Mass cytometry was used to assess the distribution of distinct groups of immune cells in the peripheral blood of treatment-naive polyarticular JIA patients and healthy controls as well as a subset of the polyarticular JIA patients in clinical remission on medication. Individual samples were debarcoded and gated for live immune cell singlets (Supplemental Figure 1; supplemental material available online with this article; https://doi.org/10.1172/jci.insight.121544DS1). Specific immune cell types were identified based on surface marker expression (Supplemental Table 4). No significant differences were identified in the distribution of any immune cell types when comparing treatment-naive patients and controls (Figure 1A). There were also no differences in cell populations detected when treatment-naive patients and remission patients were examined in aggregate or in paired treatment-naive and remission patient samples (Figure 1B). Of note, percentages of immune cell subtypes were compared rather than absolute cell counts, because cell counts were not available for the control samples.

Signaling phenotype. After examining differences in immune cell frequency between treatment-naive polyarticular JIA patients and matched controls, the baseline signaling state and signaling potential of immune cells from treatment-naive polyarticular JIA patients and matched controls was assessed. We first demonstrated that the basal and stimulated phosphorylation states of a panel of 14 signaling proteins following stimulation with 5 different cytokines were not significantly perturbed by cyropreservation during

Table 1. Patient demographics and medications

Patients	Sex	Age at sample collection (yr)	RF	CCP	ESR (mm/h)	CRP (mg/l)	Age at remission (yr)	Medications at 2nd draw	Control	Research site[A]
1	F	13.9	+	+	27	10.6	15	MTX, Plaquenil	15 yr F	1
2	F	10.3	–	–	85	138	12	MTX, Daypro	11.7 yr F	1
3	F	11.7	+	–	9	4.5	12	MTX, Enbrel	11.7 yr F	1
4	M	15	+	+	24	ND	16	MTX, Enbrel	17 yr M	1
5	M	15	+	+	14	12.2	16	MTX, Enbrel	17 yr M	1
6	M	4	–	nd	38	25.1	5	MTX, Enbrel	3 yr M	1
7	F	16.9	+	+	57	24.7			19 yr F	1
8	F	7.2	+	–	9	4			10.1 yr F	1
9	M	14.2	–	–	18	ND			15.7 yr M	1
10	F	1.5	–	nd	NA	NA	1.8	MTX	1.2 yr F	2
11	F	14.6	–	nd	NA	NA	15.3	MTX	15.4 yr F	2
12	F	11.3	–	nd	NA	NA			11.1 yr F	2
13	M	15.2	–	nd	NA	NA			9.4 yr F	2
14	F	15.8	–	nd	NA	NA	16.3	MTX, adalimumab	12.8 yr F	2
15	M	8.8	–	nd	NA	NA	9.3	MTX, tocilizumab	8.2 yr F	2
16	M	20.6	–	nd	NA	NA			5.1 yr F	2
17	M	1.4	–	nd	NA	NA			4.7 yr M	2
18									13.4 yr F	1
19									12.6 yr F	1

MTX, methotrexate; RF, rheumatoid factor; CCP, anti-cyclic citrullinated peptide; ESR, erythrocyte sedimentation rate; CRP, C-reactive protein; ND, no data; NA, not available. [A]Research sites: 1 denotes St. Louis Children's Hospital and 2 denotes Cincinnati Children's Hospital.

sample processing of a single donor (Supplemental Figure 2). To select appropriate stimuli for analysis of polyarticular JIA patients, a preliminary experiment was conducted with a single treatment-naive polyarticular JIA patient with 8 different cytokines (Supplemental Figure 3). We saw expected patterns of phosphorylation with specific cytokine stimulation. Given limitations in cell numbers, we elected to prioritize IFN-γ and IL-6 stimulation based on prior work demonstrating that IFN-γ and IL-6 were the most significantly elevated cytokines in the sera of polyarticular JIA patients (21). Due to cell number limitations, not all patient and control samples underwent stimulation with IL-6 or IFN-γ (Supplemental Table 3).

Citrus was used to quantify stratifying differences (i.e., differences that distinguish patients from controls) in signaling phenotype between treatment-naive patients and controls (or remission patients). Citrus is an analytical technique which combines hierarchical clustering of cells based on surface marker expression with an analysis of stratifying features (e.g., the signaling differences) that distinguish the two compared groups (i.e., patients and controls). As not all cells in a given population may be responding, Citrus allows for the analysis of subsets of cell populations (e.g., CD4 T cells) without the biases of manual gating. Citrus detected no distinguishing signaling differences at baseline or with IL-6 stimulation between treatment-naive patients and controls or remission patients. Differences were detected with IFN-γ stimulation between treatment-naive patients and controls as well as between treatment-naive patients and remission patients (Figure 2 and Supplemental Figures 4–6). Specifically, treatment-naive patients phosphorylated STAT3 in classical monocyte clusters ($CD14^+CD16^-HLA\text{-}DR^+$) and STAT1 and STAT3 in naive CD4 T cell clusters more strongly than controls (Figure 2). Stronger STAT3 phosphorylation in treatment-naive patients than controls was also detected on canonically gated classical monocytes via analysis with significance analysis of microarrays (SAM) (Supplemental Figure 7).

Citrus utilizes unsupervised hierarchical clustering based on surface markers, allowing distinct immune cell types to be partitioned into different parts of a hierarchical tree, facilitating analysis of stratifying characteristics of the immune cell subsets between the two groups of interest (Figure 2A and Supplemental Figure 4). There was substantial heterogeneity within the naive CD4 population and, to a lesser extent, in the classical monocytes in subsets of cells with increased IFN-γ responsiveness. To investigate differences in surface marker expression that distinguished the subsets of cells with more robust responses to IFN-γ in the patients compared with controls, trios of connected clusters in which two clusters were stratifying (between patients

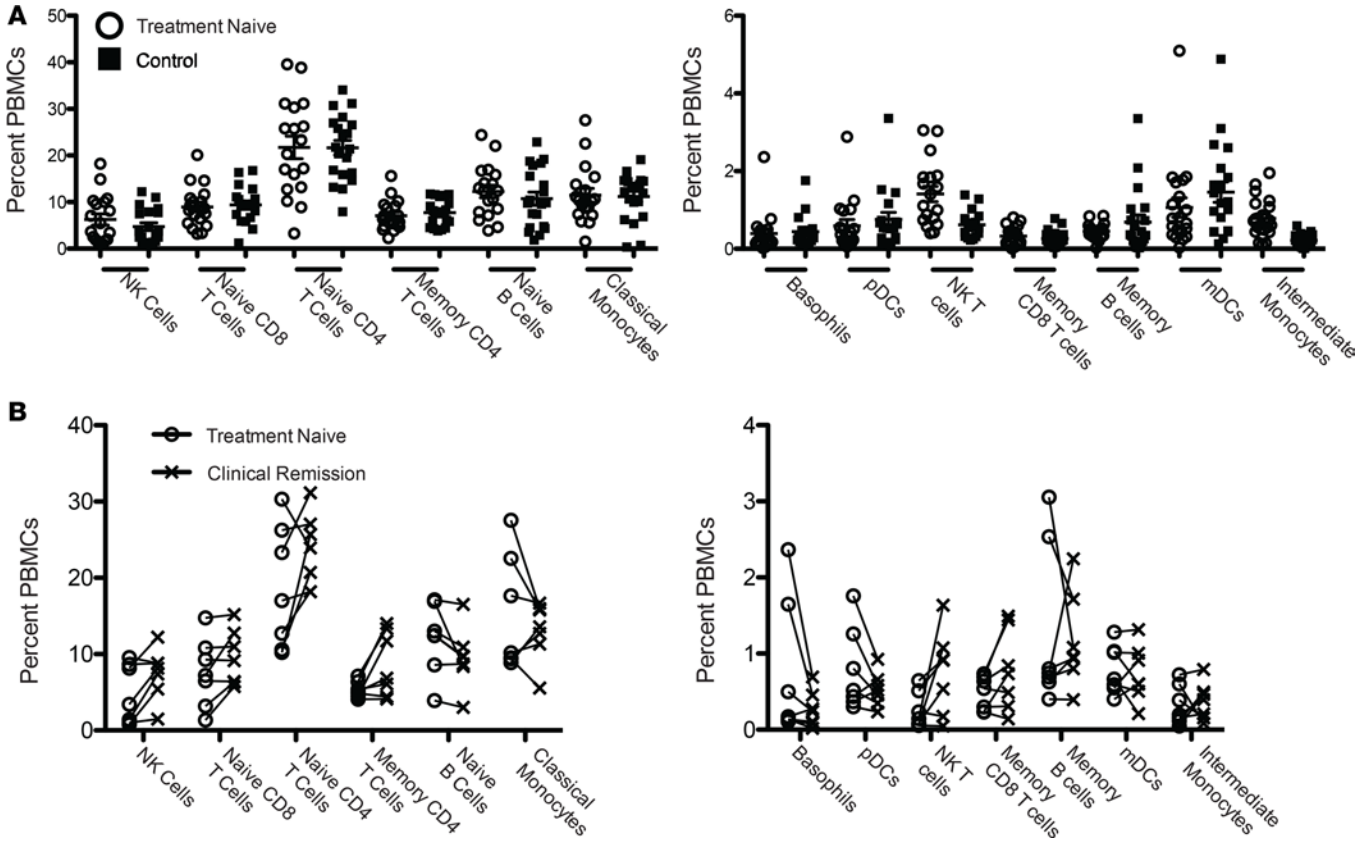

Figure 1. No differences were identified in the percentage of different cell types between treatment-naive patients and matched controls or in paired patient samples with the cessation of disease. (**A**) Treatment-naive patient versus matched control peripheral blood mononuclear cell (PBMC) percentages (1-way ANOVA [F = 52.94, $P < 0.0001$] with Bonferroni's multiple comparisons test; for pairwise comparisons, $P > 0.05$; $n = 17$ treatment-naive patients and 19 controls). Data represent mean ± SEM. (**B**) Differences for PBMC percentage in paired treatment-naive and remission patient samples (13 paired 2-tailed t tests with Benjamini Hochberg multiple hypothesis correction; $P > k/n \times 0.05$ for all comparisons, where k is the ranking from 1 to 13 of the 13 P values from lowest to highest and n is the total number of hypotheses tested ($n = 13$); $n = 7$ paired treatment-naive and remission patient samples).

and controls for both phosphorylated STAT1 [p-STAT1] and p-STAT3 in CD4 T cells) and one nonstratifying were examined. Comparisons of these trios in proximal (larger clusters) and distal (smaller clusters) parts of the tree were performed (using ANOVA with a Dunnett's post hoc test). When examining a larger, proximal CD4 cluster, the stratifying CD4 T cells had higher expression of CD11c, CD45RA (marker of naive T cells), and CD38 than the nearest nonstratifying clusters (Figure 3, A and B). When examining a smaller, more distal trio, CD45RA, CD38, and CD27 had higher expression in stratifying than nonstratifying clusters (Figure 3, A and C). A global assessment of surface marker expression patterns of stratifying and nonstratifying naive CD4 T cell clusters demonstrated that all stratifying clusters expressed CD3, CD4, and CD27, with variations in expression levels of CD4 and CD27 (Supplemental Figure 4 and Supplemental Figure 8). All stratifying clusters were $CD45RA^{+}$ and $CD38^{+}$, with CD45RA intensity decreasing and CD38 intensity increasing as clusters were divided into smaller, more specific subsets from larger clusters (Supplemental Figure 4 and Supplemental Figure 8). All stratifying clusters were $CD8^{-}$, $CD45RO^{lo}$ or $CD45RO^{-}$, and $CD56^{-}$ (Supplemental Figure 4). Comparison of surface marker intensity of all stratifying to all nonstratifying naive CD4 T cell clusters revealed a wide heterogeneity in expression of CD4, CD45RA, CD27, CD38, and HLA-DR (Supplemental Figure 8).

Heterogeneity was also observed in the stratifying classical monocyte clusters. Trios of two stratifying (between patients and controls for p-STAT3) clusters and one nonstratifying monocyte cluster revealed distinct stratifying monocyte subsets on different branches of the monocyte portion of the tree (Figure 4). In one branch of the tree, stratifying monocyte subsets had higher expression of CD45RA and HLA-DR and lower expression of CD45RO than nonstratifying clusters (Figure 4, A and B). On the other branch of the monocyte part of the tree, the nonstratifying cluster was lower in CD45RA, CD45RO, and CD11b than the largest stratifying monocyte clusters (Figure 4, A and C).

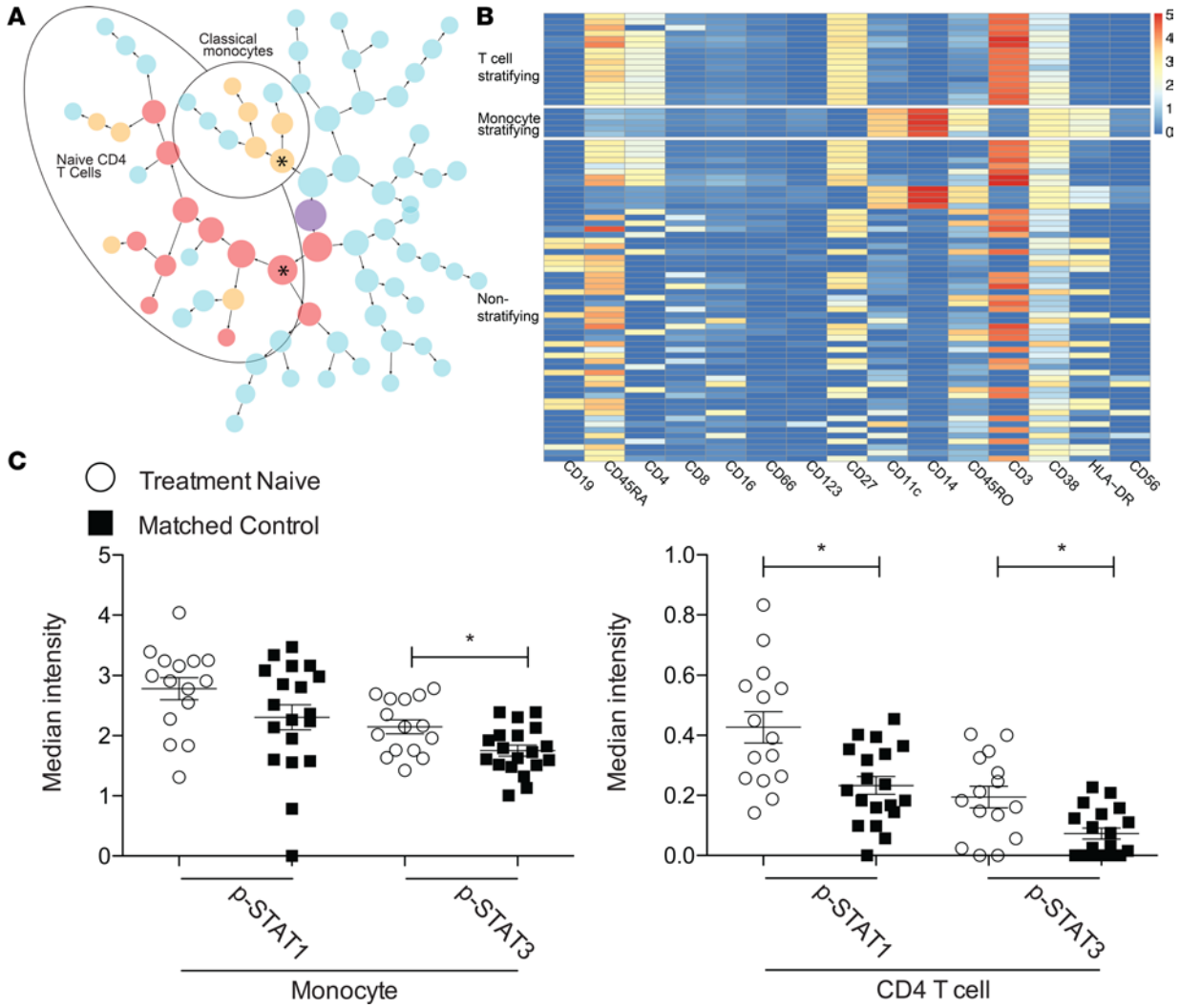

Figure 2. Classical monocyte and CD4 T cell subsets respond more strongly to IFN-γ stimulation in treatment-naive patients than controls with enhanced STAT1 and STAT3 phosphorylation. (**A**) Hierarchical clustering for IFN-γ–stimulated treatment-naive patient versus control PBMCs. Nonstratifying clusters are light blue for FDR < 0.05, p-STAT1 stratifying (different between patients and controls for a signaling molecule) clusters are purple, p-STAT3 stratifying clusters are orange, and clusters stratifying for both p-STAT1 and p-STAT3 are red. Asterisks indicate clusters visualized in **C**. (**B**) Heatmap depicting surface marker intensities for stratifying and nonstratifying classical monocyte and CD4 T cell clusters. (**C**) Arcsinh-transformed median phosphoprotein intensities for largest stratifying CD4 T cell and classical monocyte clusters (classical monocyte p-STAT1: t = 1.656, df = 32, $P = 0.108$; classical monocyte p-STAT3: t = 2.72, df = 32, $P = 0.011$; CD4 T cell p-STAT1: t = 3.04, df = 21, $P = 0.006$; CD4 T cell p-STAT3: t = 3.40, df = 32, $P = 0.002$). White circles denote treatment-naive patients, and black squares denote controls. Data represent mean ± SEM. $n = 15$ IFN-γ–stimulated treatment-naive patients, patients 4 and 5 in Table 1 did not have enough cells for an IFN-γ–stimulated sample and were excluded here; $n = 19$ controls. Statistical significance was determined with 2-tailed Student's *t* test with Benjamini-Hochberg multiple hypothesis correction to account for 4 comparisons.

All monocyte clusters were $CD14^+$, $CD11c^+$, and $CD38^+$ and $CD4^{lo}$ and lacked expression of CD8 and CD16 (Supplemental Figure 4 and Supplemental Figure 9). Comparing all stratifying to all nonstratifying classical monocyte clusters for surface marker intensity revealed trends in higher levels of median CD4, CD45RA, and HLA-DR intensity and lower levels of CD45RO intensity in stratifying than nonstratifying clusters (Supplemental Figure 9).

Similar signaling differences with IFN-γ stimulation were observed between treatment-naive patients and remission patients (Supplemental Figure 5 and Supplemental Figure 6). With IFN-γ stimulation, STAT3 was more strongly phosphorylated in some CD4 T cell clusters and STAT1 was more strongly phosphorylated in some classical monocyte clusters in treatment-naive patients in comparison to remission patients (Supplemental Figure 5, A–C). Trends toward decreasing p-STAT1 in classical monocytes and p-STAT3 in CD4 T cells were also observed paired treatment-naive and remission patient samples (Supplemental Figure 5D).

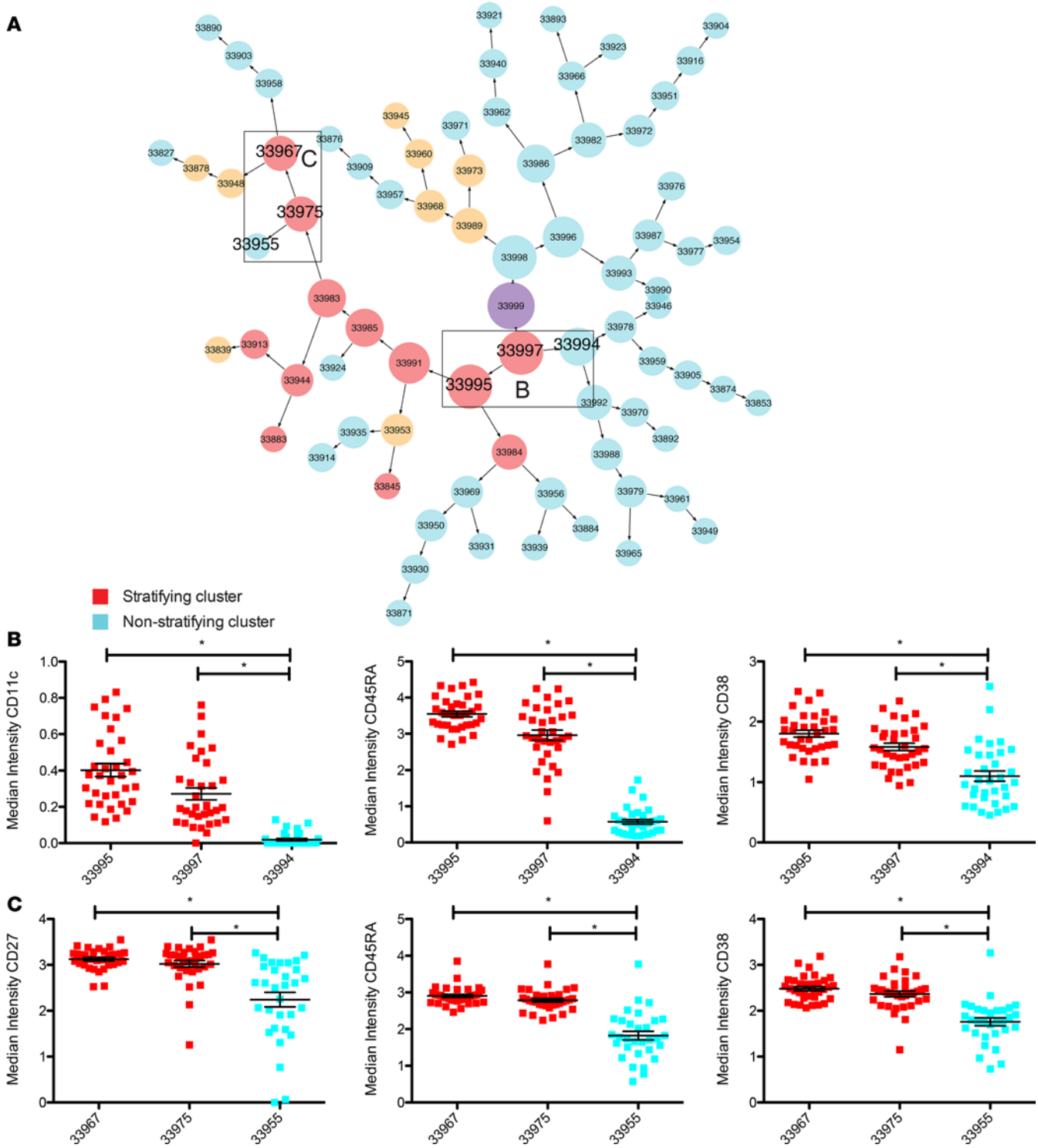

Figure 3. Heterogeneity in the naive CD4 T cells with enhanced responsiveness to IFN-γ stimulation in polyarticular JIA patients. (**A**) Schematic of hierarchical clustering computed by Citrus, with clusters analyzed in **B** and **C** denoted by boxes. Nonstratifying clusters between patient and control samples are light blue for FDR < 0.05, p-STAT1 stratifying (different between patient and control samples in regard to the phosphorylation of a specific signaling molecule) clusters are purple, p-STAT3 stratifying clusters are orange, and clusters stratifying for both p-STAT1 and p-STAT3 are red. (**B**) CD11c, CD45RA, and CD38 arcsinh-transformed medians in 3 proximal nodes in the CD4 T cell branch of clustering tree (ANOVA with Dunnett's post hoc, $*P < 0.05$). Data represent mean ± SEM. (**C**) CD27, CD45RA, and CD38 arcsinh-transformed medians in 3 distal nodes in the CD4 T cell branch of clustering tree (ANOVA with Dunnett's post hoc, $*P < 0.05$). Data represent mean ± SEM. n = 15 IFN-γ–stimulated treatment-naive patients, patients 4 and 5 in Table 1 did not have enough cells for an IFN-γ–stimulated sample and were excluded here; n = 19 controls.

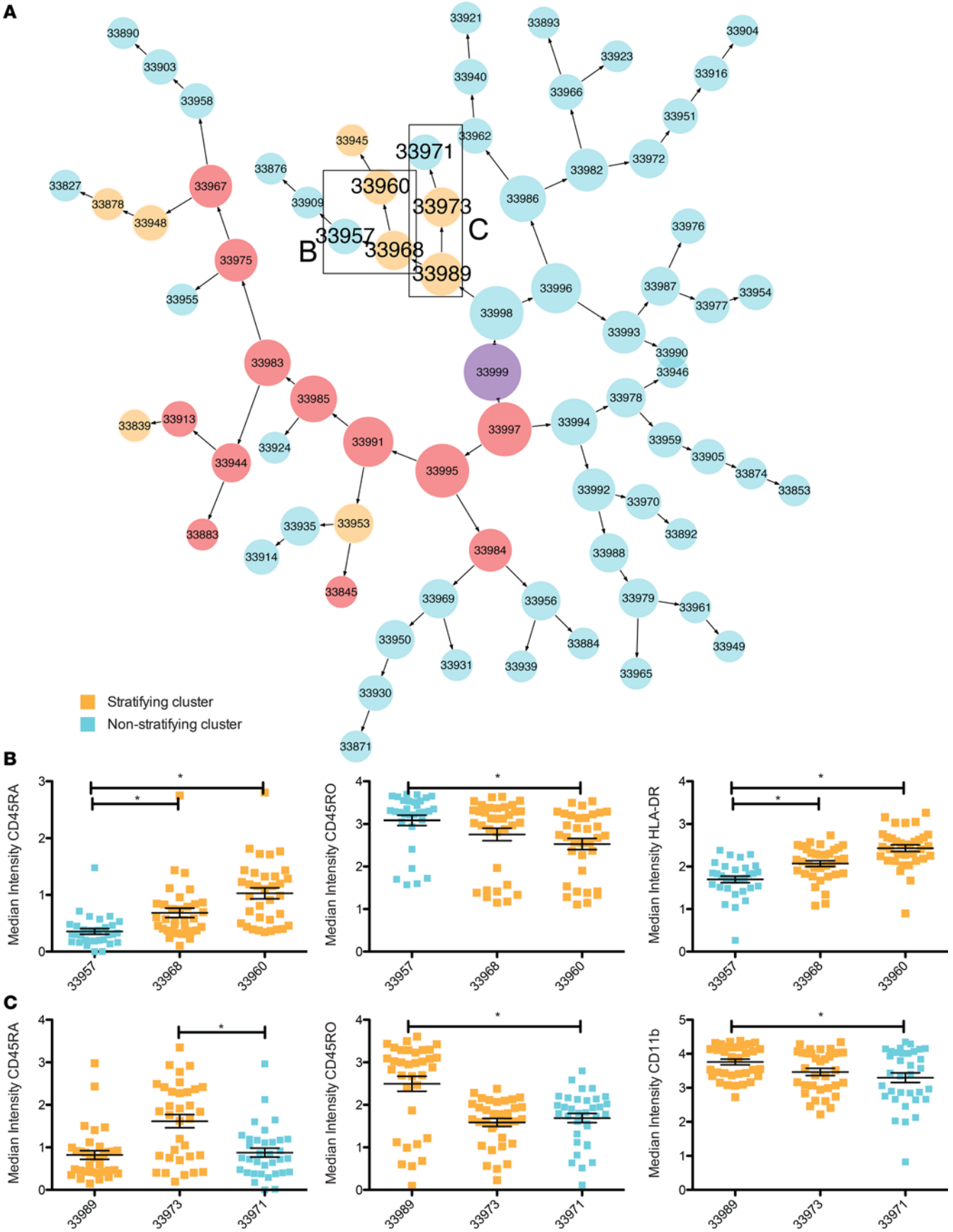
A
33890
33903
33958
33967
33827
33878
33948
33975
33955
33983
33839
33913
33944
33883
33985
33924
33991
33914
33935
33953
33845
33995
33984
33969
33950
33931
33930
33871
33956
33939
33884
33997
33998
33999
33996
33986
33909
33876
33945
33960
33957
33968
33971
33973
33989
B
C
33921
33940
33893
33966
33923
33962
33982
33904
33916
33951
33972
33976
33987
33954
33977
33993
33990
33946
33978
33994
33959
33905
33874
33853
33992
33970
33892
33988
33979
33961
33949
33965
Stratifying cluster
Non-stratifying cluster
B
Median Intensity CD45RA
Median Intensity CD45RO
Median Intensity HLA-DR
33957
33968
33960
C
Median Intensity CD45RA
Median Intensity CD45RO
Median Intensity CD11b
33989
33973
33971

Figure 4. Heterogeneity in the classical monocytes with enhanced responsiveness to IFN-γ stimulation in polyarticular JIA patients. (**A**) Schematic of hierarchical clustering computed by Citrus, with clusters analyzed in **B** and **C** denoted by boxes. Nonstratifying clusters between patient and control samples are light blue for FDR < 0.05, p-STAT1 stratifying (different between patient and control samples in regard to the phosphorylation of a specific) clusters are purple, p-STAT3 stratifying clusters are orange, and clusters stratifying for both p-STAT1 and p-STAT3 are red. (**B**) CD45RA, CD45RO, and HLA-DR arcsinh-transformed medians in one branch of monocytes in hierarchical clustering tree (ANOVA with Dunnett's post hoc, $*P < 0.05$). Data represent mean ± SEM. (**C**) CD45RA, CD45RO, and CD11b arcsinh-transformed medians in other branch of monocytes in hierarchical clustering tree (ANOVA with Dunnett's post hoc, $*P < 0.05$). Data represent mean ± SEM. n = 15 IFN-γ–stimulated treatment-naive patients, patients 4 and 5 in Table 1 did not have enough cells for an IFN-γ–stimulated sample and were excluded here; n = 19 controls.

Differences in expression of components of the IFN-γ signaling cascade. Given the differences observed in patient and control CD4 T cell and classical monocyte signaling responses, further investigation into the mechanisms contributing to differences in IFN-γ signaling was performed. Flow cytometry evaluation of targeted components of the IFN-γ signaling pathway was performed on 6 treatment-naive patients and 4 controls for whom samples were available. (Of note, half of these 6 patients had only a modest response to IFN-γ stimulation in the mass cytometry experiments.) PBMCs were stained for naive CD4 T cell or classical monocyte markers as well as p-STAT1, p-STAT3, JAK1, SOCS1, protein inhibitor of activated STAT1 (PIAS1), and IFN-γ receptor 1 (IFNGR1) in 4 separate flow cytometry panels (Supplemental Table 2). Both p-STAT1 and p-STAT3 were higher in patient compared with control naive CD4 T cells at baseline and following IFN-γ stimulation (Figure 5A). There was no difference in IFNGR1 expression between patient and control naive CD4 T cells (Figure 5B); however, JAK1 expression was higher in treatment-naive patient than control naive CD4 T cells (Figure 5C), suggesting that increased JAK1 expression may contribute to increased IFN-γ responsiveness. There was also higher expression of the inhibitory protein SOCS1 (but not PIAS1) in treatment-naive patient compared with control CD4 T cells (Figure 5D), consistent with its induction by IFN-γ as a negative regulator (28). No statistically significant differences were detected between patient and control classical monocytes in any of the examined IFN-γ signaling cascade components, perhaps reflecting the small sample size evaluated (Supplemental Figure 10).

Function in relation to phenotype. Further investigations were performed to determine whether the observed increased IFN-γ responsiveness correlated with increased naive CD4 T cell and classical monocyte proliferation in treatment-naive JIA patients. Higher levels of proliferation (analyzed as Ki-67 expression) were observed in treatment-naive patient classical monocytes and naive CD4 T cells compared with controls (Supplemental Figure 11, A and B), supporting a potential association between IFN-γ responsiveness and proliferation in treatment-naive JIA patients. Interestingly, both stratifying and nonstratifying patient classical monocytes and T cells were proliferating more than the same subsets from controls (Supplemental Figure 11, C and D).

Discussion

Despite a large number of studies focused on polyarticular JIA, the pathogenesis of this disorder is still poorly understood. This study sought to delineate signaling differences in peripheral immune cells between treatment-naive polyarticular JIA patients and controls using the high-dimensional capabilities of mass cytometry coupled with multiparameter phospho-specific antibodies. No significant differences were detected in basal signaling (unstimulated) or following IL-6 stimulation between treatment-naive JIA patients and controls (or remission patients). However, enhanced responsiveness to IFN-γ stimulation was observed with increased STAT1 and/or STAT3 phosphorylation in subsets of CD4 T cells and classical monocytes from treatment-naive JIA patients compared with controls. This enhanced responsiveness to IFN-γ correlated with increased expression of JAK1 and SOCS1 in CD4 T cells from treatment-naive JIA patients compared with controls.

No statistically significant perturbations in the percentages of different immune cells were observed between treatment-naive patients and controls or paired treatment-naive and remission patient samples. However, there was a trend toward an increase in the percentage of NK cells with cessation of active disease in the paired individual treatment-naive and remission patient samples (Figure 1B; t statistic [t] = 3.63, degrees of freedom [df] = 8, $P = 0.007$).

Unstimulated treatment-naive patients and controls did not have significantly different basal phosphorylation patterns in the mass cytometry analysis, despite reported elevated levels of IFN-γ, IL-6, and IL-1 in polyarticular JIA patient sera (21). This was unexpected given that baseline differences in

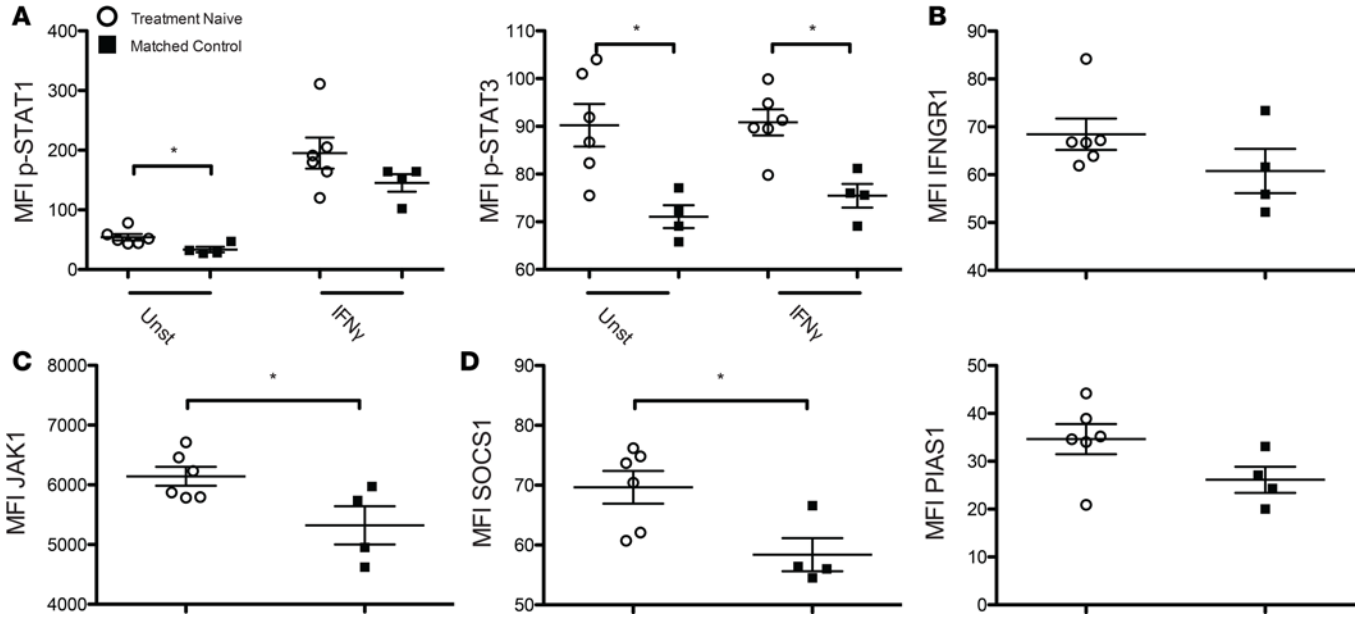

Figure 5. Signaling differences between naive CD4 T cells from treatment-naive patients and controls detected by mass cytometry are associated with higher levels of JAK1 and SOCS1 in patient naive CD4 T cells. (**A**) Differences in STAT1 phosphorylation (unstimulated: 2-tailed t = 2.71, df = 8, $P = 0.027$; stimulated: t = 1.44, df = 8, $P = 0.19$) and STAT3 phosphorylation (unstimulated: t = 3.24, df = 8, $P = 0.012$; stimulated: t = 3.91, df = 8, $P = 0.005$) in patient and control naive CD4 T cells with and without 250 ng/ml IFN-γ stimulation for 15 minutes. (**B**) IFN-γ receptor 1 (IFNGR1) in unstimulated patient and control naive CD4 T cells (t = 1.40, df = 8, $P = 0.20$). (**C**) JAK1 in unstimulated patient and control naive CD4 T cells (t = 2.56, df = 8, $P = 0.034$). (**D**) Inhibitory molecules SOCS1 (left) and protein inhibitor of activated STAT1 (PIAS1) (right) in unstimulated patient and control naive CD4 T cells (SOCS1: t = 2.78, df = 8, $P = 0.024$, PIAS1: t = 1.89, df = 8, $P = 0.096$). White circles denote treatment-naive patients, and black squares denote controls. $n = 6$ treatment-naive patients and 4 controls for which there were remaining samples available. Data represent mean ± SEM. Statistical significance was determined with Student's 2-tailed *t* tests with Benjamini-Hochberg multiple hypothesis correction, with *α = 0.05, as appropriate.

gene expression profiles have been reported in treatment-naive polyarticular JIA patients compared with healthy controls (16, 29). However, other studies of unstimulated autoimmune patient PBMCs compared with controls have also not detected baseline differences in phosphorylation of signaling molecules, including p-STAT1 and p-STAT2 in Addison's disease (30), p-ZAP70 in type 1 diabetes (31), and p-STAT1 in systemic JIA (32, 33). The lack of differences in basal phosphorylation may be due to sample processing. We evaluated parallel fresh and frozen samples from a single donor and demonstrated that cryopreservation did not affect phosphoprotein status in either unstimulated or cytokine-stimulated conditions; however, it is possible that cell processing (and removal from the serum cytokine milieu) itself alters baseline phosphorylation. The potential effect of sample processing on basal levels of phosphoproteins is consistent with previous work demonstrating differences in gene expression profiles of PBMCs after 4 hours of processing delay (34).

Signaling differences were detected between IFN-γ–stimulated treatment-naive JIA patient and control PBMCs. Naive CD4 T cells more strongly phosphorylated STAT1 and STAT3, while classical monocytes demonstrated enhanced phosphorylation of STAT3 following 15 minutes of IFN-γ stimulation of samples from treatment-naive JIA patients compared with controls. The variation observed in p-STAT1 and p-STAT3 in the treatment-naive patients was not correlated with RF status (Supplemental Figure 12). Signaling differences were also detected in these cell types when comparing treatment-naive and remission samples. These observations about enhanced responsiveness to IFN-γ stimulation are supported by prior whole blood expression profiling studies of treatment-naive polyarticular JIA patients, which found evidence of alterations in the STAT1-3/IFN response factor–mediated pathways using Ingenuity Pathway Analysis (29). Aberrant STAT3 regulation has also been inferred from pathway analysis of CD4 T cells from patients with active rheumatoid arthritis, a disease with some similarities with polyarticular JIA (35, 36). In contrast, monocytes from patients with active systemic JIA, a different subtype of JIA with an autoinflammatory phenotype, have been shown to have defective STAT1 phosphorylation following IFN-γ stimulation and elevated SOCS1 transcript expression levels (33) as well as a restricted IFN-γ–induced genetic signature and minimal upregulation of IFN-γ–induced chemokines (32).

The stratifying naive CD4 T cells and classical monocytes (i.e., subsets with increased p-STAT1 and/or p-STAT3 in patients compared with controls) were heterogeneous with varying expression levels of different surface markers. This is reminiscent of recent work using mass cytometry that demonstrated that synovial T cell infiltrates in rheumatoid arthritis were highly heterogeneous and that characterization of the CD4 T cell diversity facilitated potential discrimination of pathogenic and nonpathogenic variants of known T cell subsets (37, 38). Similarly, NK cell heterogeneity identified with mass cytometry was shown to contribute to West Nile virus susceptibility (39, 40).

While STAT1 phosphorylation is the canonical response to IFN, STAT3 phosphorylation can be coupled with STAT1 phosphorylation following IFN-γ stimulation (41). The ability of IFN-γ stimulation to phosphorylate STAT3 is demonstrated by the more pronounced and prolonged STAT3 phosphorylation following IFN-γ stimulation in murine STAT1-null cells compared with wild-type cells (41). Flow cytometry studies in a subset of our patients found that both p-STAT1 and p-STAT3 basal levels were higher in JIA patient than control naive CD4 T cells and confirmed the mass cytometry finding of increased p-STAT3 following IFN-γ stimulation. No changes in IFNGR1 or PIAS1 expression were detected via flow cytometry, but patient naive CD4 T cells had higher levels of JAK1 and SOCS1 than control cells, although the magnitude of these differences was not large. JAK1 is essential for phosphorylating STAT proteins, and elevated levels of JAK1 may contribute to a greater phosphorylation of STAT1/STAT3 in response to IFN-γ stimulation, while elevated levels of SOCS1 in patients may represent a compensatory feedback mechanism.

The enhanced STAT1 and/or STAT3 phosphorylation following IFN-γ stimulation correlated with increased CD4 T cell and classical monocyte proliferation (assessed by Ki-67 expression) in treatment-naive patients compared with controls, although CD4 T cell proliferation levels were very modest. There is evidence in murine studies that IFN-γ can enhance the proliferation and survival of CD4 T cells (42, 43). Interestingly, Ki-67 expression was higher in both stratifying and nonstratifying subsets of CD4 T cells and classical monocytes.

While insights into IFN-γ signaling differences in treatment-naive polyarticular JIA patients were gained from this work, there were several limitations, including the number of patients studied and the number of available PBMCs. The study included 17 treatment-naive samples from two centers and highlights the need for increased cooperation between centers to acquire large enough patient populations to allow new-onset, treatment-naive polyarticular JIA patients to be interrogated in a statistically meaningful manner. The number of stimulations and time points was also constrained by the sample size. Mass cytometry helps mitigate this limitation by maximizing the data extracted from small biological samples, but subtler differences in signaling may be detectable with a larger cohort and more stimulation conditions and time points.

This study highlights the utility of mass cytometry coupled with multiparameter phospho-specific antibodies in analyzing signal differences in small-volume patient samples. Using this approach, differences in STAT1 and/or STAT3 phosphorylation in subsets of CD4 T cells and classical monocytes following IFN-γ stimulation were identified in treatment-naive polyarticular JIA patient compared with control samples. The enhanced responsiveness of CD4 T cells to IFN-γ stimulation correlated with increased expression of JAK1 and SOCS1 in treatment-naive JIA patients. These results suggest that drugs that attenuate IFN-γ signaling (e.g., JAK inhibitors) may be useful in treating polyarticular JIA patients and provide a potential mechanistic rationale for anecdotal observations regarding the effectiveness of JAK inhibitors in refractory polyarticular JIA patients (including the case series of 3 refractory polyarticular JIA patients treated with tofacitinib, a JAK inhibitor, in the Supplemental Data) and for an ongoing clinical trial (NCT02591434) of tofacitinib in polyarticular JIA patients. Interestingly, one of patients in the case series (case 2) was included in the mass cytometry analysis as a treatment-naive sample (patient 7 in Table 1), and a follow up sample was subsequently obtained while the patient was in clinical remission on tofacitinib (after completion of the initial analysis). Naive CD4 T cell p-STAT1 and p-STAT3 following IFN-γ stimulation were lower in the remission sample while on tofacitinib (as well as leflunomide and hydroxychloroquine) compared with the paired treatment-naive samples (Supplemental Figure 13). Future studies will focus on more detailed interrogation of specific $CD45RA^+$ CD4 T cell subsets to help us further understand mechanistically the increased IFN-γ responsiveness in subsets of CD4 T cells in this disease.

Methods

Patient cohort. Polyarticular JIA patients diagnosed in our pediatric rheumatology clinics were eligible for enrollment if they were new onset and treatment naive. Samples were also collected from 10 of the patients after achieving clinical remission, as defined by the Wallace criteria (without the use of erythrocyte sedimentation rate [ESR] or C-reactive protein [CRP]). The Wallace criteria define clinical remission as having no joints with active arthritis; physician global assessment of disease activity indicating clinical disease quiescence; no active uveitis; no fever, splenomegaly, rash, serositis, or generalized lymphadenopathy; and normal ESR or CRP (8). Seven of the seventeen treatment-naive patients had either not achieved clinical remission at the time of the study analysis or had no available follow-up samples. PBMCs from treatment-naive polyarticular JIA patients and controls were also utilized from the Cincinnati Children's Hospital Medical Center Pediatric Rheumatology Tissue Repository and the Cincinnati Genomic Control Cohort. Given the relatively small number of treatment-naive polyarticular JIA patients in this study and recent evidence demonstrating minimal differences in microarray data between RF^+ and RF^- polyarticular JIA PBMCs (29), we did not further subset our polyarticular JIA patients into RF^+ and RF^- patients.

Reagents. Antibodies conjugated to heavy metals were purchased from Fluidigm, with the exception of CD69 (Biolegend, Supplemental Table 1). Antibodies for flow cytometry were purchased from multiple vendors (Supplemental Table 2).

Sample preparation and collection. Blood samples were collected from 17 treatment-naive, new-onset polyarticular JIA patients; a follow-up sample was collected when 10 of the 17 JIA patients were in clinical remission on medication; and samples were collected from 19 controls (Table 1), and PBMCs were isolated using a Ficoll gradient (GE Healthcare) and cryopreserved.

Mass cytometry. PBMCs were thawed and stained with cisplatin to discriminate dead cells (Fluidigm). Cells were aliquoted (1.7×10^6 to 3.3×10^6 cells/tube) in 1-ml total volume and rested for 30 minutes at 37°C prior to simulation. Cells were either left unstimulated or were stimulated with 50 ng/ml IL-6 or 250 ng/ml IFN-γ (PBL) for 15 minutes in RPMI1640 supplemented with 10% fetal calf serum at 37°C, fixed with MaxPar Fix I Buffer (Fluidigm), permeabilized with MaxPar Barcode Perm Buffer (Fluidigm), and barcoded with the Cell-ID 20-Plex Barcoding Kit (Supplemental Table 3; Fluidigm). Barcoded samples were pooled and stained with antibodies for surface markers. After staining for surface markers, the pooled samples were methanol permeabilized and stained with antibodies for intracellular markers (Supplemental Table 1). Samples were incubated with Cell-ID Intercalator-Ir (Fluidigm) to detect debris and doublets, and run on a CyTOF2/Helios instrument (Fluidigm). Samples were debarcoded using the Single Cell Debarcoder, a stand-alone MATLAB application (44). Data were analyzed using Cytobank and R. A run control from the same normal donor was used in each experiment to normalize the phosphoprotein data as follows:

$asinh(x_{sample}/5) - asinh(x_{Run\ Control}/5)$, where x represents raw median signaling intensity for each phosphorylated signaling molecule in a specific immune cell subset and *asinh* represents the inverse hyperbolic sine.

Citrus. Citrus, a computational technique combining hierarchical clustering with an analysis of stratifying differences in cluster features (in our case, phosphorylation of a panel of signaling proteins within specific immune cells) between two groups of samples, was performed with the R "citrus" package on fcs files gated on live immune cells to compare treatment-naive patients with matched controls (or remission samples) under different stimulation conditions (45). Surface markers were clustering parameters. Minimum cluster size was set as 2% of the total population with 10,000 events sampled per file. Cluster characterization features were signaling molecules. All clustering and characterization features were arcsinh transformed. Differences in cluster features were calculated using SAM. A FDR of 5% was set as a cutoff for significance ($q < 0.05$).

To delineate which subsets of cells responded differently between treatment-naive patients and controls, deeper analysis of surface markers on stratifying (significantly different signaling molecule phosphorylation between patients and controls for a given cluster) versus nonstratifying clusters for p-STAT1 and p-STAT3 was performed. All surface markers were analyzed. A trio of clusters containing three connected nodes in which there were two stratifying clusters and one nonstratifying cluster were examined to determine which surface markers contribute to a cluster being stratifying or nonstratifying. Surface marker intensity for clusters was also visualized as a colored hierarchical clustering tree as well as plots of median surface marker intensity for all stratifying and nonstratifying classical monocyte and naive CD4 T cell clusters.

Flow cytometry. To further investigate potential mechanisms causing differences in IFN-γ signaling potential, flow cytometry experiments were performed with a subset of 6 treatment-naive patients (for which there were remaining samples available) and 4 control samples from the samples collected at the host site. Samples (0.5×10^6 to 1×10^6 cells/sample) were left unstimulated or stimulated 15 minutes with 250 ng/ml IFN-γ and fixed with BD Cytofix/Cytoperm buffer. Samples were stained with one of several antibody panels (Supplemental Table 2). Flow cytometry was performed on a 12-color LSRFortessa X-20 Flow Cytometer (BD) and analyzed with FlowJo (FlowJo). Classical monocytes and naive CD4 T cells were gated and analyzed for differences in components of the IFN-γ signaling cascade between patient and control samples.

Statistics. One-way ANOVA with Bonferroni's multiple comparisons test between all patient and control samples was used to test differences in the distribution of immune cell subsets between treatment-naive patients and controls (46). A paired 2-tailed Student's *t* test with Benjamini-Hochberg multiple hypothesis correction was used to analyze paired treatment-naive and remission patient immune cell percentages. SAM was used to explore differences in signaling phenotype in various types of PBMCs. Differences detected by SAM were confirmed with unpaired 2-tailed Student's *t* tests and Benjamini-Hochberg multiple hypothesis correction. To determine which PBMC subsets drove differences detected in SAM, live cells were analyzed via Citrus with SAM to classify differences distinguishing patients and controls, and results were confirmed using unpaired 2-tailed Student's *t* tests with Benjamini-Hochberg multiple hypothesis correction. Differences in surface marker expression between trios of clusters with two stratifying and one nonstratifying were analyzed with ANOVA and a Dunnett's test in relation to a singular nonstratifying cluster. Classical monocyte and naive CD4 T proliferation differences were tested for both gated populations and Citrus clusters with an unpaired 2-tailed Student's *t* test and Benjamini-Hochberg multiple hypothesis correction. To analyze flow cytometry data, 2-tailed Student's *t* tests with Benjamini-Hochberg multiple hypothesis correction were used to test the hypotheses that there are differences in STATs (p-STAT1 and p-STAT3), IFNGR1, JAK1, and inhibitory proteins in cells (SOCS1 and PIAS1). An α value of 0.05 was used to determine significant *P* values with multiple hypothesis correction as appropriate.

Study approval. This work was approved by the institutional review boards at Washington University School of Medicine and Cincinnati Children's Hospital. Polyarticular JIA was defined according to the International League Against Rheumatism criteria for classifying idiopathic arthritis of childhood (22). Written informed consent was received from participants prior to inclusion in the study.

Author contributions

The manuscript was written by AAT, ABO, and ARF. The manuscript was edited by AAT, HM, ABO, JTP, TLG, HLM, ALD, ONM, DJL, SDT, AAG, MAC, STO, and ARF. Reagents and/or samples were provided by MAC, HM, SDT, DJL, and AAG. Research studies were designed by AAT, HLM, ONM, STO, and ARF. Experiments were conducted by AAT, JTP, TLG, HLM, ALD, and ONM. Data were analyzed and interpreted by AAT, HLM, and ARF.

Acknowledgments

We would like to thank our patients for their participation, without which this work would not be possible. We would also like to thank David Hunstad and Josh Alinger for their critical readings of this manuscript. Technical support was provided by the Immunomonitoring Laboratory, which is supported by the Andrew M. and Jane M. Bursky Center for Human Immunology and Immunotherapy Programs. This research was supported by a Rheumatology Research Foundation Disease Targeted Research Pilot Grant (to ARF) and the National Institute of Allergy and Infectious Diseases (R01 AI078994 to ARF) as well as the National Institute of Arthritis and Musculoskeletal and Skin Diseases (NIAMS) (P01 AR048929 to SDT and P30 AR070549 to SDT). Cincinnati Children's Hospital Medical Center Pediatric Rheumatology Tissue Repository was supported by NIAMS P01 AR048929 and P30 AR070549. The Cincinnati Genomic Control Cohort was supported in part by the Cincinnati Children's Research Foundation and its Cincinnati Genomic Control Cohort. HM was supported in part by the NIH (P01 AR048929, P30 AR070549, R01 HD089928, and U01 AI130830).

Address correspondence to: Anthony R. French, Department of Pediatrics, Washington University, Box 8208, 660 South Euclid Avenue, St. Louis, Missouri 63110, USA. Phone: 314.286.2885; Email: french_a@wustl.edu.

1. Macaubas C, Nguyen K, Milojevic D, Park JL, Mellins ED. Oligoarticular and polyarticular JIA: epidemiology and pathogenesis. *Nat Rev Rheumatol*. 2009;5(11):616–626.
2. Oberle EJ, Harris JG, Verbsky JW. Polyarticular juvenile idiopathic arthritis - epidemiology and management approaches. *Clin Epidemiol*. 2014;6:379–393.
3. Peterson LS, Mason T, Nelson AM, O'Fallon WM, Gabriel SE. Juvenile rheumatoid arthritis in Rochester, Minnesota 1960-1993. Is the epidemiology changing? *Arthritis Rheum*. 1996;39(8):1385–1390.
4. Mason T, et al. Frequency of abnormal hand and wrist radiographs at time of diagnosis of polyarticular juvenile rheumatoid arthritis. *J Rheumatol*. 2002;29(10):2214–2218.
5. Mason T, Reed AM, Nelson AM, Thomas KB. Radiographic progression in children with polyarticular juvenile rheumatoid arthritis: a pilot study. *Ann Rheum Dis*. 2005;64(3):491–493.
6. Oen K, Malleson PN, Cabral DA, Rosenberg AM, Petty RE, Cheang M. Disease course and outcome of juvenile rheumatoid arthritis in a multicenter cohort. *J Rheumatol*. 2002;29(9):1989–1999.
7. Fantini F, Gerloni V, Gattinara M, Cimaz R, Arnoldi C, Lupi E. Remission in juvenile chronic arthritis: a cohort study of 683 consecutive cases with a mean 10 year followup. *J Rheumatol*. 2003;30(3):579–584.
8. Wallace CA, Huang B, Bandeira M, Ravelli A, Giannini EH. Patterns of clinical remission in select categories of juvenile idiopathic arthritis. *Arthritis Rheum*. 2005;52(11):3554–3562.
9. Shoop-Worrall SJW, et al. How common is clinically inactive disease in a prospective cohort of patients with juvenile idiopathic arthritis? The importance of definition. *Ann Rheum Dis*. 2017;76(8):1381–1388.
10. Guzman J, et al. The risk and nature of flares in juvenile idiopathic arthritis: results from the ReACCh-Out cohort. *Ann Rheum Dis*. 2016;75(6):1092–1098.
11. Davies R, Gaynor D, Hyrich KL, Pain CE. Efficacy of biologic therapy across individual juvenile idiopathic arthritis subtypes: A systematic review. *Semin Arthritis Rheum*. 2017;46(5):584–593.
12. Prahalad S, Shear ES, Thompson SD, Giannini EH, Glass DN. Increased prevalence of familial autoimmunity in simplex and multiplex families with juvenile rheumatoid arthritis. *Arthritis Rheum*. 2002;46(7):1851–1856.
13. Prahalad S, Glass DN. A comprehensive review of the genetics of juvenile idiopathic arthritis. *Pediatr Rheumatol Online J*. 2008;6:11.
14. Hinks A, et al. Dense genotyping of immune-related disease regions identifies 14 new susceptibility loci for juvenile idiopathic arthritis. *Nat Genet*. 2013;45(6):664–669.
15. Jarvis JN, et al. Gene expression profiling in neutrophils from children with polyarticular juvenile idiopathic arthritis. *Arthritis Rheum*. 2009;60(5):1488–1495.
16. Jiang K, Sawle AD, Frank MB, Chen Y, Wallace CA, Jarvis JN. Whole blood gene expression profiling predicts therapeutic response at six months in patients with polyarticular juvenile idiopathic arthritis. *Arthritis Rheumatol*. 2014;66(5):1363–1371.
17. Wouters CH, Ceuppens JL, Stevens EA. Different circulating lymphocyte profiles in patients with different subtypes of juvenile idiopathic arthritis. *Clin Exp Rheumatol*. 2002;20(2):239–248.
18. Zhou J, Tang X, Ding Y, An Y, Zhao X. Natural killer cell activity and frequency of killer cell immunoglobulin-like receptors in children with different forms of juvenile idiopathic arthritis. *Pediatr Allergy Immunol*. 2013;24(7):691–696.
19. Griffin TA, et al. Gene expression signatures in polyarticular juvenile idiopathic arthritis demonstrate disease heterogeneity and offer a molecular classification of disease subsets. *Arthritis Rheum*. 2009;60(7):2113–2123.
20. De Benedetti F, Robbioni P, Massa M, Viola S, Albani S, Martini A. Serum interleukin-6 levels and joint involvement in polyarticular and pauciarticular juvenile chronic arthritis. *Clin Exp Rheumatol*. 1992;10(5):493–498.
21. de Jager W, Hoppenreijs EP, Wulffraat NM, Wedderburn LR, Kuis W, Prakken BJ. Blood and synovial fluid cytokine signatures in patients with juvenile idiopathic arthritis: a cross-sectional study. *Ann Rheum Dis*. 2007;66(5):589–598.
22. Lovell DJ, et al. Etanercept in children with polyarticular juvenile rheumatoid arthritis. Pediatric Rheumatology Collaborative Study Group. *N Engl J Med*. 2000;342(11):763–769.
23. Lovell DJ, et al. Adalimumab with or without methotrexate in juvenile rheumatoid arthritis. *N Engl J Med*. 2008;359(8):810–820.
24. Quartier P, et al. A multicentre, randomised, double-blind, placebo-controlled trial with the interleukin-1 receptor antagonist anakinra in patients with systemic-onset juvenile idiopathic arthritis (ANAJIS trial). *Ann Rheum Dis*. 2011;70(5):747–754.
25. Ruperto N, et al. Two randomized trials of canakinumab in systemic juvenile idiopathic arthritis. *N Engl J Med*. 2012;367(25):2396–2406.
26. Lovell DJ, et al. Long-term safety and efficacy of rilonacept in patients with systemic juvenile idiopathic arthritis. *Arthritis Rheum*. 2013;65(9):2486–2496.
27. Brunner HI, et al. Efficacy and safety of tocilizumab in patients with polyarticular-course juvenile idiopathic arthritis: results from a phase 3, randomised, double-blind withdrawal trial. *Ann Rheum Dis*. 2015;74(6):1110–1117.
28. Ilangumaran S, Rottapel R. Regulation of cytokine receptor signaling by SOCS1. *Immunol Rev*. 2003;192:196–211.
29. Jiang K, et al. Whole blood expression profiling from the TREAT trial: insights for the pathogenesis of polyarticular juvenile idiopathic arthritis. *Arthritis Res Ther*. 2016;18(1):157.
30. Edvardsen K, et al. Peripheral blood cells from patients with autoimmune addison's disease poorly respond to interferons in vitro, despite elevated serum levels of interferon-inducible chemokines. *J Interferon Cytokine Res*. 2015;35(10):759–770.
31. Nervi S, et al. Specific deficiency of p56lck expression in T lymphocytes from type 1 diabetic patients. *J Immunol*. 2000;165(10):5874–5883.
32. Sikora KA, Fall N, Thornton S, Grom AA. The limited role of interferon-γ in systemic juvenile idiopathic arthritis cannot be explained by cellular hyporesponsiveness. *Arthritis Rheum*. 2012;64(11):3799–3808.
33. Macaubas C, et al. Altered signaling in systemic juvenile idiopathic arthritis monocytes. *Clin Immunol*. 2016;163:66–74.
34. Barnes MG, Grom AA, Griffin TA, Colbert RA, Thompson SD. Gene expression profiles from peripheral blood mononuclear cells are sensitive to short processing delays. *Biopreserv Biobank*. 2010;8(3):153–162.
35. Ye H, et al. CD4 T-cell transcriptome analysis reveals aberrant regulation of STAT3 and Wnt signaling pathways in rheumatoid arthritis: evidence from a case-control study. *Arthritis Res Ther*. 2015;17:76.
36. Meshaal S, El Refai R, El Saie A, El Hawary R. Signal transducer and activator of transcription 5 is implicated in disease activity

in adult and juvenile onset systemic lupus erythematosus. *Clin Rheumatol*. 2016;35(6):1515–1520.
37. Rao DA, et al. Pathologically expanded peripheral T helper cell subset drives B cells in rheumatoid arthritis. *Nature*. 2017;542(7639):110–114.
38. Fonseka CY, Rao DA, Raychaudhuri S. Leveraging blood and tissue CD4+ T cell heterogeneity at the single cell level to identify mechanisms of disease in rheumatoid arthritis. *Curr Opin Immunol*. 2017;49:27–36.
39. Yao Y, et al. The natural killer cell response to West Nile virus in young and old individuals with or without a prior history of infection. *PLoS One*. 2017;12(2):e0172625.
40. Strauss-Albee DM, et al. Human NK cell repertoire diversity reflects immune experience and correlates with viral susceptibility. *Sci Transl Med*. 2015;7(297):297ra115.
41. Qing Y, Stark GR. Alternative activation of STAT1 and STAT3 in response to interferon-gamma. *J Biol Chem*. 2004;279(40):41679–41685.
42. Reed JM, Branigan PJ, Bamezai A. Interferon gamma enhances clonal expansion and survival of CD4+ T cells. *J Interferon Cytokine Res*. 2008;28(10):611–622.
43. Wallace CA, et al. American College of Rheumatology provisional criteria for defining clinical inactive disease in select categories of juvenile idiopathic arthritis. *Arthritis Care Res (Hoboken)*. 2011;63(7):929–936.
44. Zunder ER, et al. Palladium-based mass tag cell barcoding with a doublet-filtering scheme and single-cell deconvolution algorithm. *Nat Protoc*. 2015;10(2):316–333.
45. Bruggner RV, Bodenmiller B, Dill DL, Tibshirani RJ, Nolan GP. Automated identification of stratifying signatures in cellular subpopulations. *Proc Natl Acad Sci USA*. 2014;111(26):E2770–E2777.
46. Benjamini Y, Hochberg Y. Controlling the false discovery rate - a practical and powerful approach to multiple testing. *J Roy Stat Soc B Met*. 1995;57(1):289–300.